**Diacylglycerol kinase ζ inhibits Gαq-induced atrial remodeling in transgenic mice**

Masamichi Hirose [a], Yasuchika Takeishi [b], Takeshi Niizeki [c], Hisashi Shimojo [d], Tsutomu Nakada [a], Isao Kubota [c], Jun Nakayama [d], Ulrike Mende [e], Mitsuhiko Yamada [a]

a) Department of Molecular Pharmacology, Shinshu University School of Medicine, Nagano 390-8621, Japan
b) The First Department of Internal Medicine, Fukushima Medical School, Fukushima, Japan Yasuchika Takeishi takeishi@fmu.ac.jp
c) Department of Cardiology, Pulmonology, and Nephrology Yamagata University School of Medicine, Yamagata 990-9585, Japan.
d) Department of Pathology, Shinshu University School of Medicine, Nagano 390-8621, Japan.
e) Cardiovascular Research Center, Division of Cardiology, Rhode Island Hospital & The Warren Alpert Medical School of Brown University, Providence, RI, USA.

Address correspondence to Masamichi Hirose, M.D., Department of Molecular Pharmacology, Shinshu University School of Medicine, Matsumoto, Nagano 390-8621 Japan

Phone No. 81-263-37-2606

Fax No. 81-263-37-3085

E-mail: mhirose@shinshu-u.ac.jp

Short running title: Hirose et al. DAGζ-induced prevention of atrial remodeling

Conflict of interest statement: There are no potential conflicts of interest.

**Abstract**

**BACKGROUND** Our previous study demonstrated that diacylglycerol kinase ζ (DGKζ), which degenerates diacylglycerol (DAG), inhibits ventricular structural remodeling and rescues activated G protein αq (Gαq)-induced heart failure. However, whether DGKζ inhibits atrial remodeling is still unknown.

**OBJECTIVE** This study aimed to elucidate **e**ffects of DGKζ on atrial remodeling.

**METHODS** A transgenic mouse (Gαq-TG) with cardiac expression of activated Gαq and a double transgenic mouse (Gαq/DGKζ-TG) with cardiac overexpression of DGKζ and activated Gαq were created.

**RESULTS** During electrocardiogram (ECG) recording for 10 min, atrial fibrillation was observed in 5 of 11 anesthetized Gαq-TG mice but not in any wild type (WT) and Gαq/DGKζ-TG mice ($p< 0.05$). All of the ECG parameters measured were prolonged in the Gαq-TG compared with WT mice. Interestingly, in Gαq/DGKζ-TG mice, while the PR and RR intervals were still prolonged, the P interval, QRS complex, and QT interval were not different from those in WT mice. In Langendorff-perfused hearts, the incidence of atrial tachyarrhythmia induced by rapid atrial pacing was greater in Gαq-TG hearts than in Gαq/DGKζ-TG hearts ($p<0.05$). Action potential duration prolongation and impulse conduction slowing were observed in Gαq-TG atria compared with Gαq/DGKζ-TG atria. Dilatation of the left atrium with thrombus formation was observed in 9 Gαq-TG hearts but not in any Gαq/DGKζ-TG hearts. Moreover, the degree of extensive interstitial fibrosis in the left atrium was greater in Gαq-TG hearts than that in Gαq/DGKζ-TG hearts ($p<0.05$).

CONCLUSION These results demonstrate that DGKζ inhibits Gαq-induced atrial remodeling and suggest that DGKζ is a novel therapeutic target for AF.

Key words: atrial fibrillation, atrial remodeling, G protein coupled receptor, mouse heart, transgenic mouse, diacylglycerol kinase, optical mapping, atrial arrhythmias

Abbreviation

AF, atrial fibrillation; DAG, diacylglycerol; $IP_{3,}$ inositol 1,4,5-trisphosphate; WT mouse, wild type mouse; Gαq-TG mouse, a transgenic mouse with cardiac expression of activated-Gαq; Gαq/DGKζ-TG mouse, a double transgenic mouse with cardiac overexpression of DAG kinaseζ and the activated-Gαq; GPCR, Gαq protein-coupled receptor; APD, action potential duration; CV, conduction velocity; AT, atrial tachyarrhythmia; High PAC, high incidence of premature atrial contraction

**Introduction**

Atrial fibrillation (AF) is the most common arrhythmia in clinical practice. AF is associated with a wide range of potential morbidity and mortality. Our understanding of AF pathophysiology has advanced significantly through an increased awareness of the role of atrial electrical and structural remodeling. Many forms of atrial remodeling promote the occurrence or maintenance of AF by acting on the fundamental arrhythmia mechanisms.[1] The Gαq protein-coupled receptor (GPCR) signaling pathway plays a critical role in the development of cardiac hypertrophy and congestive heart failure. GPCR agonists such as angiotensin II, endothelin-1 stimulate phospholipace C, leading to diacylglycerol (DAG) and inositol 1,4,5-trisphosphate ($IP_3$) production. DAG activates protein kinase C, and IP3 causes intracellular $Ca^{2+}$ release, both of which may promote remodeling in the heart.[1-4] One major route for terminating DAG signaling is thought to be its phosphorylation and inactivation by DAG kinase (DGK), producing phosphatidic acid.[5-8] We recently generated transgenic mice with cardiac specific overexpression of DGKζ using an α-myosin heavy chain promoter and demonstrated that DGKζ negatively regulated the hypertrophic signaling cascade and resultant ventricular remodeling in response to GPCR agonists.[9] In addition, Niizeki et al.[10] have demonstrated that DGKζ inhibits ventricular structural remodeling and rescues Gαq-induced heart failure. However, whether DGKζ inhibits atrial remodeling is still unknown. The objective of this study is to elucidate effects of DGKζ on atrial remodeling using a transgenic mouse with transient cardiac expression of activated Gαq[11] and a double transgenic mouse with cardiac-specific overexpression of both DAG kinase (DGK) ζ and the activated Gαq.[10]

## Methods

The experimental protocol was approved by the institutional animal experiments committee and complied with the *Guide for Care and Use of Laboratory Animals* published by the US National Institutes of Health (NIH publication 85-23, revised 1996).

### Animals.

A transgenic mouse (Gαq-TG mouse) with transient cardiac expression of activated G protein αq and a double transgenic mouse (Gαq/DGKζ-TG mouse) with cardiac-specific overexpression of both DAG kinase (DGK) ζ and the activated Gαq were used in the present study.[10, 11] The genotypes of the wild-type (WT), Gαq-TG, Gαq/DGKζ-TG mice were identified by polymerase chain reaction (PCR) with the use of tail genomic DNA as previously reported.

### Electrocardiography (ECG)

Age-matched WT (n = 10), Gαq-TG (n = 11), and Gαq/DGKζ-TG (n = 13) female mice were anesthetized with sodium pentobarbital (30 mg/kg) applied intraperitoneally. ECG lead II was recorded and filtered (0.1 to 300 Hz), digitized with 12-bit precision at a sampling rate of 1000 Hz per channel (Microstar Laboratories Inc., Bellevue, WA, USA), and transmitted into a microcomputor and saved to CD-ROM.

### Langendorff-perfused mouse heart

After ECG lead II recording, all of mice were treated with sodium heparin (500 USP units/kg i.v.). After a midline sternal incision, hearts were quickly excised and connected to a modified Langendorff apparatus. A polyterafluoroethylene-coated silver unipolar

electrode was used to stimulate the epicardial surface of left atrial appendage at twice diastolic threshold current with a duration of 1 msec. Each preparation was perfused under constant flow conditions with oxygenated (95% oxygen, 5% $CO_2$) Tyrode's solution containing in mM: NaCl, 141.0; KCl, 5.0; $CaCl_2$, 1.8; $NaHCO_3$, 25.0; $MgSO_4$, 1.0; $NaH_2PO_4$, 1.2; HEPES, 5; and dextrose, 5.0 (pH of 7.4 at $36 \pm 1^{o}$C). Perfusion pressure was measured with a pressure transducer (Nihon Kohden Co, Tokyo, Japan) and maintained within a pressure range (50-60 mmHg) by adjusting flow. Preparations were stained with 5 μl of voltage sensitive dye, di-4-ANEPPS (Molecular Probes, Eugene, OR, USA) dissolved in 0.19 ml of ethanol at a concentration of 8 mM. Cardiac rhythm was monitored using 3 silver disk electrodes fixed to the chamber in positions corresponding to ECG limb leads II. The ECG signals were filtered (0.3 to 300 Hz), amplified (1000 x), and displayed on a digital recorder. Perfusion pressure and flow were continuously monitored during each experiment. After each experiment, tissue viability was confirmed by 2 ml of 2,3,5-tetrazolium chloride (TTC, 14 mg/ml) staining.

**Optical mapping system**

Beating and perfused hearts were immersed in a Tyrode's-filled custom-built chamber specifically designed for optical recordings. In every experiment, the mapping field was positioned at the left atrial free wall. The optical mapping system used in this study has been described in detail elsewhere.[12] Briefly, excitation light (510 nm) obtained from a 250 W quartz tungsten halogen lamp (Oriel Co. Stratford, CT, USA) was directed to the heart using a liquid light guide. Fluoresced light from the heart was collected by a tandem lens assembly and directed to a long pass filter (>630 nm) that passes light of longer

wavelengths to a 16X16 element photodiode array. Signals recorded from each photodiode and ECG signals were multiplexed and digitized with 12-bit precision at a sampling rate of 3000 Hz per channel (Microstar Laboratories Inc., Bellevue, WA, USA). An optical magnification of 3X was used, corresponding to a mapping field of 0.6 cm x 0.6 cm and 0.37 mm spatial resolution between recording pixels. To view, digitize, and store anatomical features, a mirror was temporarily inserted between the lenses of the tandem lens assembly to direct reflected light to a digital video camera (DCR-PC120 Sony Co. Tokyo, Japan).

**Experimental protocol**

First, after anesthesia ECG lead II was recorded for 10 min in all mice. Second, to measure action potential duration (APD) and conduction velocity (CV), optical action potentials were recorded for 10 sec from the left atrial free walls at a basic cycle length of 150 ms in isolated Langendorff-perfused hearts. Third, rapid atrial pacing at a pacing cycle length of 80-100 ms for approximately 5 sec from the left atrial appendage was performed to induce atrial tachyarrhythmia (AT). AT was defined as a rapid (cycle length <100 ms) regular or irregular rhythm persisting more than five beats. When rapid pacing induced AT that terminated spontaneously within 1 min, AT was reinitiated at the same cycle length. Each experiment ended after rapid pacing was performed ten times or when rapid pacing induced AT lasting more than 1 min. Optical action potentials were recorded during the AT from the epicardial surface of left atrial free wall for 10 sec.

**Data analysis**

In all anesthetized mice, P, PR, QRS complex, QT, and RR interval were measured

from ECG lead II. High incidence of premature atrial contraction (High PAC) was defined as PAC occurring more than 10 beats/min. Atrial fibrillation (AF) was defined as an irregularly irregular rhythm without P waves. In all Langendorff hearts, left atrial size was measured from the distance between upper and bottom end of the left atrium as described in figure 3A. In all optical action potentials, automated algorithms were used to determine depolarization time relative to a single fiducial point (i.e., the stimulus). Depolarization time was defined as the point of maximum positive derivative in the action potential upstroke ($dV/dt_{max}$). Depolarization contour maps were computed for the entire mapping field. Repolarization time was defined as the time when repolarization reached a level of 80 %. The APD was defined as the difference between repolarization time and depolarization time. Mean optical APD at the left atrial free wall was calculated from the average of optical APDs at more than 10 sites. The method of Bayly[13] was modified for optically recorded action potential maps to accurately quantify the direction and magnitude of CV at each recording site. Mean CV was calculated from the average of local conduction velocities at more than 10 sites as described before.[12] All data are shown as the mean ± SE. An analysis of variance with Bonferroni's test was used for the statistical analysis of multiple comparisons of data. Fisher's exact test was used to compare the incidence of AF between different conditions. $P < 0.05$ was considered statistically significant.

**Gross anatomy and histology**

After Langendorff heart experiment ended, the heart was fixed with a 30 % solution of formalin in phosphate-buffered saline at room temperature for more than 24 hours, embedded in paraffin, and then cut serially from the apex to the base. Six sections were

stained with hematoxylin/eosin or Masson's trichrome for histopathological analysis. To assess the degree of fibrosis, digital microscopic images were taken from the sections stained with Masson's trichrome stain using light microscopy with digital camera system. Morphometry was carried out with image analyzing software MacSCOPE (MITANI Corporation, Tokyo), on a Macintosh computer. The measurements were performed on 3 images from different points of the left atrial free wall in each preparation. Connective and myocardial tissue was differentiated on the basis of their color, respectively. The fibrosis fraction was obtained by calculating the ratio of total connective area to total myocardial area from 3 images in each preparation.

## Results

### Arrhythmia induction in anesthetized mice

Shown in figure 1 are representative ECGs recorded from three different types of mouse (WT, Gαq-TG, Gαq/DGKζ-TG mice). Upper 2 ECGs show atrial arrhythmias recorded from Gαq-TG mice. In case 1, PAC was observed. In case 2, the ECG demonstrated disorganized and irregular RR interval without P waves, which are ECG features of AF. In contrast, lower 2 ECGs recorded from a WT and Gαq/DGKζ-TG mouse showed P wave and QRS complex with regular RR interval without any arrhythmia, indicating sinus rhythm. In addition, sinus cycle length in Gαq TG mice and Gαq/DGKζ-TG mouse was longer compared with that in WT mouse. Table 1 shows overall data of atrial arrhythmia induction. Atrial arrhythmias were never observed in WT mice. In contrast, atrial arrhythmias including AF were observed in 9 of 11 Gαq-TG mice. Interestingly, the arrhythmias were observed in only 2 of 13 Gαq/DGKζ-TG mice and AF was significantly inhibited in Gαq/DGKζ-TG mice compared with Gαq-TG mice.

### ECG parameters in anesthetized mice

Table 2 shows overall data of electrophysiological parameters in 3 different types of mice. All of ECG parameters measured prolonged in Gαq-TG mice compared with WT mice. Interestingly, while the PR and RR interval still prolonged in Gαq/DGKζ-TG mice compared with WT mice, the P interval, QRS complex and QT interval were not different from WT mice in Gαq/DGKζ-TG mice.

**Left atrial APD and CV**

Shown in figure 2A are representative examples of optical action potentials recorded from the left atrial free wall in three different types of heart during steady state pacing at a cycle length of 150 msec. Atrial APD prolongation was observed in a Gαq-TG heart compared with WT and Gαq/DGKζ-TG heart. Mean APD significantly prolonged in Gαq-TG left atria compared with WT and Gαq/DGKζ-TG left atria (Fig. 2B). Shown in figure 2C are representative examples of activation isochrone maps recorded from the left atrial free wall during steady state pacing at a cycle length of 150 ms in three different types of heart. Relative crowding of isochrone lines in the Gαq-TG heart (Fig. 2C, middle) indicates conduction slowing when compared with the WT and Gαq/DGKζ-TG heart (Fig. 2C, left and right). In addition, when considering all experiments (Fig. 2D), mean CV on the left atrial free wall was significantly slower in Gαq-TG hearts compared with the WT and Gαq/DGKζ-TG hearts.

**Induction of AT in Langendorff-perfused heart**

Before rapid pacing, spontaneous AT was not induced in any Langendorff-perfused WT and Gαq/DGKζ-TG hearts. In addition, even though rapid pacing was performed, AT was induced in none of WT hearts and in 2 of 13 Gαq/DGKζ-TG hearts. In contrast, spontaneous AT was induced in 3 of 11 Gαq-TG hearts before rapid pacing. Moreover, rapid pacing induced AT in 7 of 11 Gαq-TG hearts tested. The incidence of AT induction by rapid pacing significantly greater in the Gαq-TG hearts than in the Gαq/DGKζ-TG hearts ($p < 0.05$, Fisher's exact test). Shown in figure 2E is an example of spontaneous AT in a Langendorff-perfused Gαq-TG heart. Representative atrial and ventricular optical signals during AT showed rapid repetitive activation in only atrium at a cycle length of less than 70 ms without pacing.

**Left atrial size, thrombus, and fibrosis**

Shown in figure 3A are shows representative examples of Langendorff perfused Gαq and Gαq/DGKζ-TG hearts. The left atrium was enlarged in the Gαq-TG heart (5.9 mm) compared with Gαq/DGKζ-TG heart (2.8 mm). Figure 3B shows overall data of left atrial size. The left atrial size/body weight ratio was increased in Gαq-TG hearts compared with WT heart. In Gαq/DGKζ-TG hearts, the ratio was not different from WT heart. On gross examination of four-chamber section of the heart, all chambers are dilated in a Gαq TG heart compared with a WT and Gαq/DGKζ-TG heart, and mural thrombus was found in the left atrium in the Gαq TG heart (Fig. 4A left). Histologically, the thrombus showed varying degrees of organization (Fig. 4A right). Layers of the degenerated blood cells and fibrin with granulation tissue and fibrosis, which attaches thrombus widely to the endocardium, were observed. The thrombus was observed in 9 of 11 Gαq TG hearts but not in any WT and Gαq/DGKζ-TG hearts. Moreover, extensive interstitial fibrosis in the left atrium was observed in Gαq-TG hearts compared with a WT and Gαq/DGKζ-TG heart (Fig. 4B). The degree of myocardial fibrosis in the left atrium was significantly greater in Gαq-TG mice than in WT and Gαq/DGKζ-TG mice (Fig. 4C) (fibrosis fraction: 48.2 ± 3.4 vs 12.1 ± 2.1 %, $p < 0.05$).

**Discussion**

In this study, we found that the overexpression of DGKζ in the hearts of Gαq-TG mice prevents the generation of atrial arrhythmias including AF. We also found that DGKζ inhibits atrial electrical and structural remodeling (APD prolongation, impulse conduction slowing, left atrial enlargement, increased left atrial fibrosis, and left atrial thrombus). These results suggest that the activation of DAG contributes to atrial remodeling and the generation of AF.

In this study, DGKζ inhibited the incidence of ectopic foci such as PAC to trigger AF and also prevented spontaneous AF. Recently, it has been demonstrated that activation of DAG pathway stimulates several transient receptor cation channels.[14] In addition, a study has suggested that activation of DAG and/or protein kinase C (PKC) stimulates calcium-activated nonselective cation channel particularly in the setting of hypertrophy and heart failure.[15] It could be implicated in the generation of cardiac arrhythmias because activation of these cannels can promote cell depolarization. In fact, Thandroyen et al.[16] have reported that a calcium-activated nonselective cation channel is involved in the transient inward current responsible for delayed afterdepolarizations. Moreover, it has been shown that PKC potentiates L-type calcium currents which increase calcium influx through the channels[17] and inhibits potassium channels, such as the delayed rectifier[18], suggesting calcium overload in myocardium which leads to triggering events. Our previous study demonstrated that the expression and subcellular translocation of PKC increased in Gαq TG mice. In addition, the prolongation of atrial APD was observed in Gαq TG mice compared with WT and Gαq/DGKζ-TG mice. These results suggest that the activation of

DAG pathway can contribute to the generation of arrhythmias.

Activation of the GPCR signaling pathway in atrium directly promotes atrial remodeling,[1] whereas it may also promote atrial remodeling through left ventricular dysfunction and heart failure induced by the activation of the GPCR signaling pathway in ventricle.[19-21] In fact, atrial electrical and structural remodeling, such as action potential prolongation, interstitial fibrosis, and chamber dilatation, has been seen in patients with heart failure[22] and animal models of pacing induced heart failure.[21, 23] With atrial fibrosis, conduction abnormalities results in an increase in AF vulnerability.[21] Our previous study has demonstrated that Gαq TG mice exhibits the upregulation of fetal gene induction such as atrial natriuretic factor (ANF), brain natriuretic peptide (BNP), and beta-MHC, and prominent perivascular and interstitial fibrosis in the left ventricle.[10] In addition, chamber dilatation, cardiac dysfunction, and heart failure as shown by increased left ventricular end-diastoric pressure, reduced +dP/dt, -dP/dt and prolonged Tau were also observed in Gαq TG mice compared with WT and Gαq/DGKζ-TG mice. Four chambers dilatation was also observed in the present study (Fig. 4A). Therefore, atrial remodeling such as atrial fibrosis and dilatation might also be induced through the left ventricular dysfunction and heart failure in this model. In the previous study,[10] it has also been demonstrated that DGKζ inhibits ventricular structural remodeling and rescues Gαq-induced heart failure. Thus, DGKζ may also inhibit the atrial remodeling through the improvement of heart failure.

Gαq TG mice activate $IP_3$ and DAG pathway, whereas they also activate another intra-cellular signaling pathways including the mitogen-activated protein kinase pathway

(MAPK), the janus kinase/signal transducers and activators of transcription pathway (JAK/STAT), and Src-family pathway.[1, 24] These signaling pathways are known to promote cellular hypertrophy, to stimulate fibroblast proliferation, and to activate matrix protein synthesis leading to tissue fibrosis.[1, 24] Electrophysiological remodeling in atrium may also be associated with activation of some of these pathways. Therefore, several signal pathways independent of $IP_3$ and DAG pathway might participate in atrial electrical and structural remodeling in this model. Moreover, our Gαq TG mice have a possibility to stimulate local secretion of angiotensin II and those signal pathways because of chronic atrial stretch in the setting of heart failure.[25, 26] Our previous study has demonstrated that phosphorylation activities of MAP kinase increased in Gαq TG mice compared with WT and Gαq/DGKζ-TG mice.[10] Nevertheless, overexpression of DGKζ in the hearts of Gαq-TG mice inhibited atrial electrical and structural remodeling. These results suggest that DAG pathway contributes to atrial remodeling in this model.

It is well known that reentry can induce AF. Reentry requires a suitable vulnerable substrate. Atrial remodeling has the potential to increase the likelihood of reentrant activity through the suitable vulnerable substrate. For example, electrophysiogical remodeling, such as the refractory period shortening (ie. APD shortening) and slowing of impulse conduction, can promote reentry.In this study, however, impulse conduction slowing was observed in Gαq-TG left atria, but the APD shortening was not. Therefore, the wavelength of reentry calculated from APD and CV was similar between Gαq-TG and Gαq/DGKζ-TG atrium. However, AF was never induced in Gαq/DGKζ-TG. Structural remodeling, such as trial enlargement and extensive interstitial fibrosis, was also observed in Gαq-TG compared with Gαq/DGKζ-TG hearts. Atrial dimensions are a particularly important determinant of

occurrence of reentry.[1] Moreover, the extensive interstitial fibrosis which interferes with impulse conduction is favor to promote AF in heart failure.[21] Therefore, although our result did not demonstrate the occurrence of reentry in Gαq-TG atria DGKζ induced-inhibition of left atrial enlargement and interstitial fibrosis (i.e. inhibition of structural remodeling) might perticipate in preventing AF induced in Gαq-TG mice.

**References**


1. Nattel, S, Burstein B, Dobrev D. Atrial remodeling and atrial fibrillation: Mechanisms and implication. Circ Arrhythmia Electrophysiol 2008;1:62-73.
2. Matsumoto Y, Aihara H, Yamauchi-Kohno R, et al. Long-term endothelin A receptor blockade inhibits electrical remodeling in cardiomyopathic hamsters. Circulation 2002;106:613-619.
3. Domenighetti AA, Boixel C, Cefai D, et al. Chronic angiotensin II stimulation in the heart produces an acquired long QT syndrome associated with IK1 potassium current downregulation. J Mol Cell Cardiol 2007;42:63-70.
4. Fischer R, Dechend R, Gapelyuk A, et al. Schirdewan, Angiotensin II-induced sudden arrhythmic death and electrical remodeling. Am J Physiol 2007;293:H1242-H1253.
5. Goto K, Kondo H, A 104-kDa diacylglycerol kinase containing ankyrin-like repeats localizes in the cell nucleus. Proc Natl Acad Sci USA 1996;93:11196-11201.
6. Goto K, Kondo H, Diacylglycerol kinase in the central nervous system: Molecular heterogeneity and gene expression. Chem Phys Lipids 1999;98:109-117.
7. Topham MK, Bunting M, Zimmerman GA, et al. Protein kinase C regulates the nuclear localization of diacylglycerol kinase-zeta. Nature 1998;394:697-700.
8. Topham MK, Prescott SM, Mammalian diacylglycerol kinases, a family of lipid kinases with signaling functions. J Biol Chem 1999;274:11447-11450.
9. Arimoto T, Takeishi Y, Takahashi H, et al. Cardiac-specific overexpression of diacylglycerol kinase zeta prevents Gq protein-coupled receptor agonist-induced cardiac hypertrophy in transgenic mice. Circulation 2006;113:60-66.
10. Niizeki T, Takeishi Y, Kitahara T, et al. Diacylglycerol kinase ζ rescues Gαq-induced heart failure in transgenic mice. Circ J 2008;72:309-317.

11. Mende U, Kagen A, Cohen A, et al. Transient cardiac expression of constitutively active Gαq leads to hypertrophy and dilated cardiomyopathy by calcineurin-dependent and independent pathways. Proc Natl Acad Sci USA 1998;95:13893-13898.
12. Hirose M, Takeishi Y, Miyamoto, et al. Mechanism for atrial tachyarrhythmia in chronic volume overload-induced dilated atria. J Cardiovasc Electrophysiol 2005;16:1-10.
13. Bayly PV, KenKnight BH, Rogers JM, et al. Estimation of conduction velocity vector fields from epicardial mapping data. IEEE. Trans. Biomed. Eng. 45 (1998) 563-571.
14. Nilius B, Qwsianik G, Voets T et al. Transient receptor potential cation channels in disease. Physiol Rev 2007;87:165-217.
15. Guinamard R, Chatelier A, Lenfant J et al. Activation of the Ca2+-activated nonselective cation channel by diacylglycerol analogues in rat cardiomyocytes. J Cardiovasc Electrophysiol 2004;15:342-348.
16. Thandroyen FT, Morris AC, Habler HK et al. Intracellular calcium transients and arrhythmias in isolated heart cells. Circ Res 1991;69:810-819.
17. O-Uchi J, Sasaki H, Morimoto S et al. Interaction of α1-adrenoceptor subtypes with different G proteins induces opposite effects on cardiac L-type $Ca^{2+}$ Channel. Circ Res 2008;102:1378-1388.
18. Clement-Chomienne O, Walsh M, Cloe W. Angiotensin II activation of protein kinase C decreases delayed rectifier K+ current in rabbit vascular myocyes. J Physiol (Lond) 1996;495:689-700.
19. Lipp P, Laine M, Tovey SC, et al. Functional $InsP_3$ receptors that may modulate excitation–contraction coupling in the heart. Curr Biol. 12000;10:939–942.

20. Mackenzie L, Bootman MD, Laine M, et al. The role of inositol 1,4,5-trisphosphate receptors in $Ca^{2+}$ signalling and the generation of arrhythmias in rat atrial myocytes. J Physiol 2002;541:395–409.

21. Li D, Fareh S, Leung TK, et al. Promotion of atrial fibrillation by heart failure in dogs: atrial remodeling of a different sort. Circulation 1999;100:87-95.

22. Sanders P, Morton JB, Davidson NC et al. Electrical remodeling of the atria in conjestive heart failure: electrophysiological and electroanatomic mapping in humans. Circulation 2003;108:1461-1468.

23. Shi Y, Ducharme A, Li D, Gaspo R et al. Remodeling of atrial dimensions and emptying function in canine models of atrial fibrillation. Cardiovasc Res 2001;52:217-225.

24. Goette A, Lendeckel U, Klein HU. Signal transduction systems and atrial fibrillation. Cardiovasc Res 2002;54:247-258.

25. Ruwhof C, van der Laarse A. Mechanical stress-induced cardiac hypertrophy: mechanisms and signal transduction pathways. Cardiovasc Res 2000;47**:**23–37.

26. Sadoshima J, Izumo, S. The cellular and molecular response of cardiac myocytes to mechanical stress. Annu Rev Physiol 1997;59:551–571.

**Figure Legends**

Figure 1. ECG lead II recordings from three different types of mouse (WT, Gαq TG and Gαq/DGKζ-TG mouse). Upper 2 ECGs show atrial arrhythmias (PAC, premature atrial contraction; AF, atrial fibrillation) in anesthetized Gαq TG mice. Lower 2 ECGs recorded from WT and Gαq/DGKζ-TG mice showed P wave and QRS complex with regular RR interval without any arrhythmia, indicating sinus rhythm. Sinus cycle length in Gαq TG mice and Gαq/DGKζ-TG mouse was longer compared with that in WT mouse. See text for details.

Figure 2. Action potential duration (APD) and conduction velocity (CV) recorded from the left atrial free wall in three different types of mouse (WT, Gαq TG and Gαq/DGKζ-TG mouse). Panel A: Representative examples of optical action potentials recorded from the left atrial free wall in three different types of mouse during steady state pacing at a cycle length of 150 ms. Panel B: Mean APD calculated from local APD at more than 10 sites. Mean APD was significantly prolonged in Gαq-TG left atria compared with WT and Gαq/DGKζ-TG left atria. Panel C: Representative examples of activation isochrone maps from the left atrial free wall during steady state pacing at a cycle length of 150 ms in three different types of mouse. Activation maps are shown with 2-ms isochrones. Panel D: Mean CV calculated from local CV at more than 10 sites. Mean CV on the left atrial free wall was significantly slower in Gαq-TG hearts compared with the WT and Gαq/DGKζ-TG hearts. See text for details. $^{*}p < 0.05$ vs. values in WT mice; $^{\$}p < 0.05$ vs. values in Gαq TG mice. The numbers in parentheses indicate the number of observations at each of

three different types of mice. Age and gender were matched among three different types of mice. Panel E: An example of spontaneous atrial tachyarrhythmia (AT) in a Langendorff-perfused Gαq-TG heart. See text for details.

Figure 3. Left atrial size measured from Langendorff-perfused heart. Panel A: Representative examples of Langendorff perfused Gαq and Gαq/DGKζ-TG hearts. Left atrial size was measured from the distance between upper end and bottom end of the left atrium. The left atrium was enlarged in the Gαq-TG heart (5.9 mm) compared with Gαq/DGKζ-TG heart (2.8 mm). Panel B: Overall data of left atrial size. Left atrial size/BW ratio was increased in Gαq-TG hearts compared with WT heart and the ratio was back to normal levels in Gαq/DGKζ-TG hearts. $^{*}p < 0.05$ vs. values in WT mice; $^{\$}p < 0.05$ vs. values in $G_{\alpha q}$ TG mice. The numbers in parentheses indicate the number of observations at each of three different types of mice. Age and gender were matched among three different types of mice. BW, body weight.

Figure 4 Gross examination of four-chamber section of a heart and its histology. Panel A: Gross examination of four-chamber section of a heart and its histology stained with hematoxylin/eosin in a WT, Gαq-TG and Gαq/DGKζ-TG heart. Original magnification: x 1.25 and x 40 Panel B: Histology of the left atrium stained with Masson's trichrome in a WT, Gαq-TG and Gαq/DGKζ-TG heart. Original magnification: x 20 and x 40. Panel C: Comparison of the fibrosis fraction in the left atrium in WT, Gαq-TG and Gαq/DGKζ-TG mice. $^{*}p < 0.05$ vs. values in WT mice; $^{\$}p < 0.05$ vs. values in $G_{\alpha q}$-TG mice. The numbers in parentheses indicate the number of observations at each of three different types of mice.

Age and gender were matched among three different types of mice. See text for details.

Table 1 Incidence of spontaneously induced cardiac arrhythmias in three different types of anesthetized mice

| | WT | $G_{\alpha q}$ TG | $G_{\alpha q}$ /DGK$\zeta$ TG |
|---|---|---|---|
| n | 10 | 11 | 13 |
| Age (week) | 36 ± 4 | 34 ± 3 | 30 ± 1 |
| High PAC (>10/min) | 0/10 | 7/11[a] | 2/13[$] |
| AF | 0/10 | 5/11[a] | 0/13[$] |
| Any arrhythmia | 0/10 | 9/11[a] | 2/13[$] |

High incidence of premature atrial contraction (High PAC) was defined as PACs occurring more than 10 beats/min. [a]$p < 0.05$ vs. values in WT; [$]$p < 0.05$ vs. values in $G_{\alpha q}$ TG. (Fisher's exact test) WT, wild type mice.

Table 2 Electrophysiological parameters in three different types of anesthetized mice

| Parameters | WT | $G_{\alpha q}$ TG | $G_{\alpha q}$ /DGKζ |
|---|---|---|---|
| TG | (n = 10) | (n = 11) | (n = 13) |
| P (msec) | 17 ± 1 | 24 ± 1 [a] | 18 ± 1 [$] |
| RR (msec) | 137 ± 5 | 163 ± 10 [a] | 160 ± 8 [a] |
| PR (msec) | 37 ± 2 | 68 ± 7 [a] | 55 ± 5 [a] |
| QRS (msec) | 16 ± 0.3 | 18 ± 1 [a] | 15 ± 0.3 [$] |
| QT (msec) | 35 ± 1 | 46 ± 4 [a] | 34 ± 1 [$] |

Each value represents the mean ± S.E. [a] $p < 0.05$ vs. values in WT; [$] $p < 0.05$ vs. values in $G_{\alpha q}$ TG mice. WT, wild type mice.

**Fig. 1**

**Fig. 2**

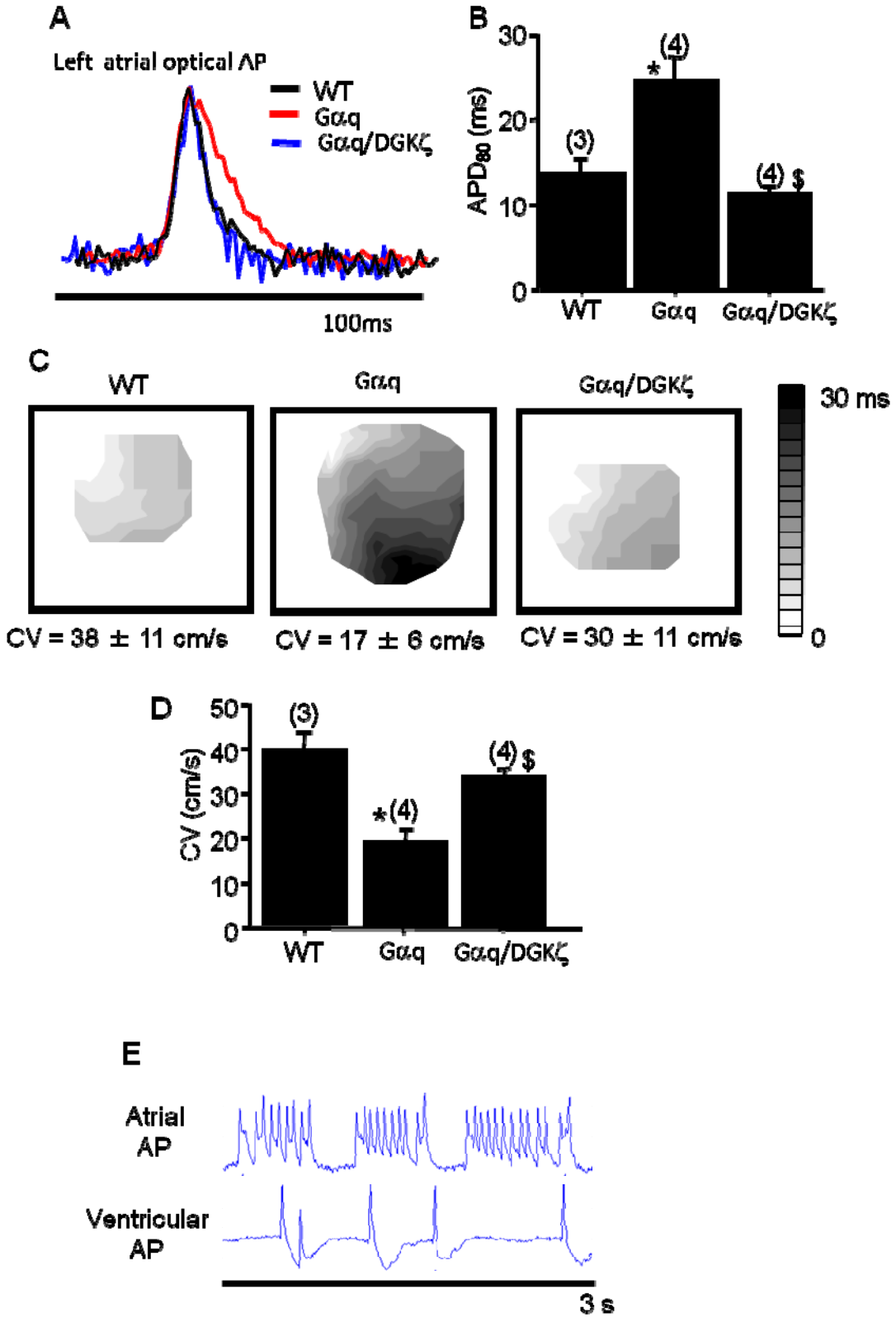
A
Left atrial optical AP
WT
Gαq
Gαq/DGKζ
100ms
B
APD80 (ms)
30
20
10
0
(3)
*(4)
(4) $
WT
Gαq
Gαq/DGKζ
C
WT
Gαq
Gαq/DGKζ
30 ms
0
CV = 38 ± 11 cm/s
CV = 17 ± 6 cm/s
CV = 30 ± 11 cm/s
D
CV (cm/s)
50
40
30
20
10
0
(3)
*(4)
(4) $
WT
Gαq
Gαq/DGKζ
E
Atrial AP
Ventricular AP
3 s

**Fig. 3**

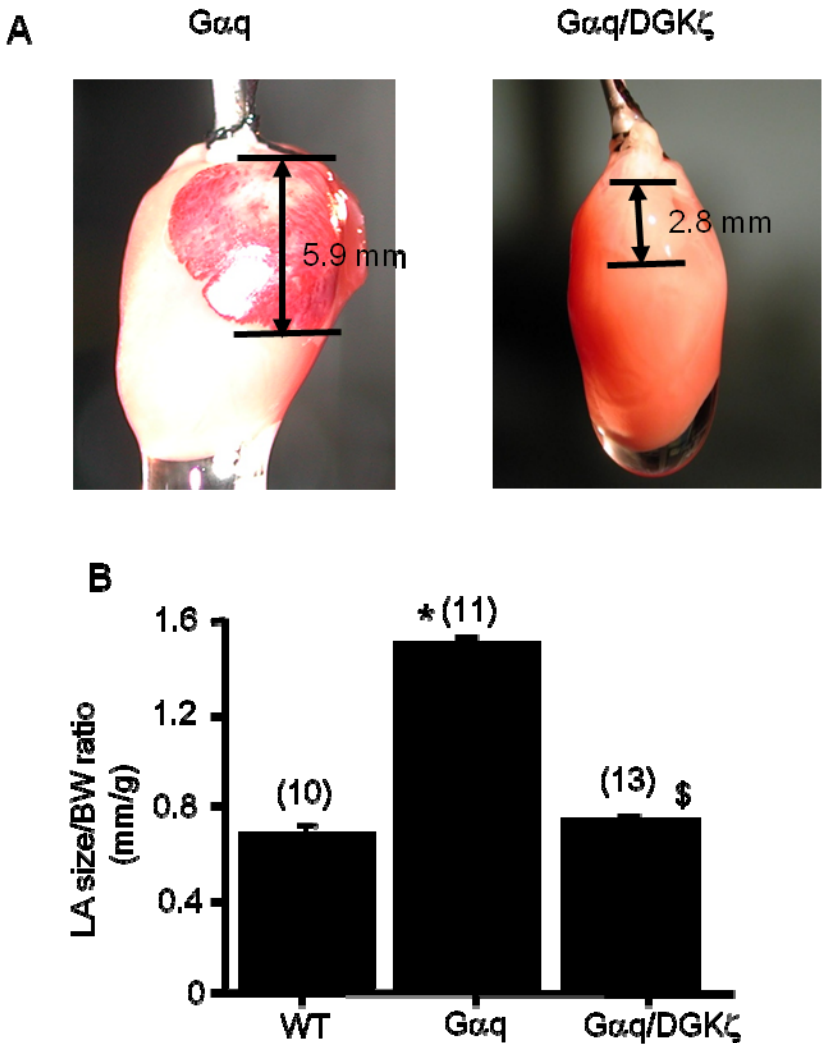
A
Gαq
Gαq/DGKζ
5.9 mm
2.8 mm
B
LA size/BW ratio (mm/g)
1.6
1.2
0.8
0.4
0
(10)
*(11)
(13) $
WT
Gαq
Gαq/DGKζ

**Fig. 4**

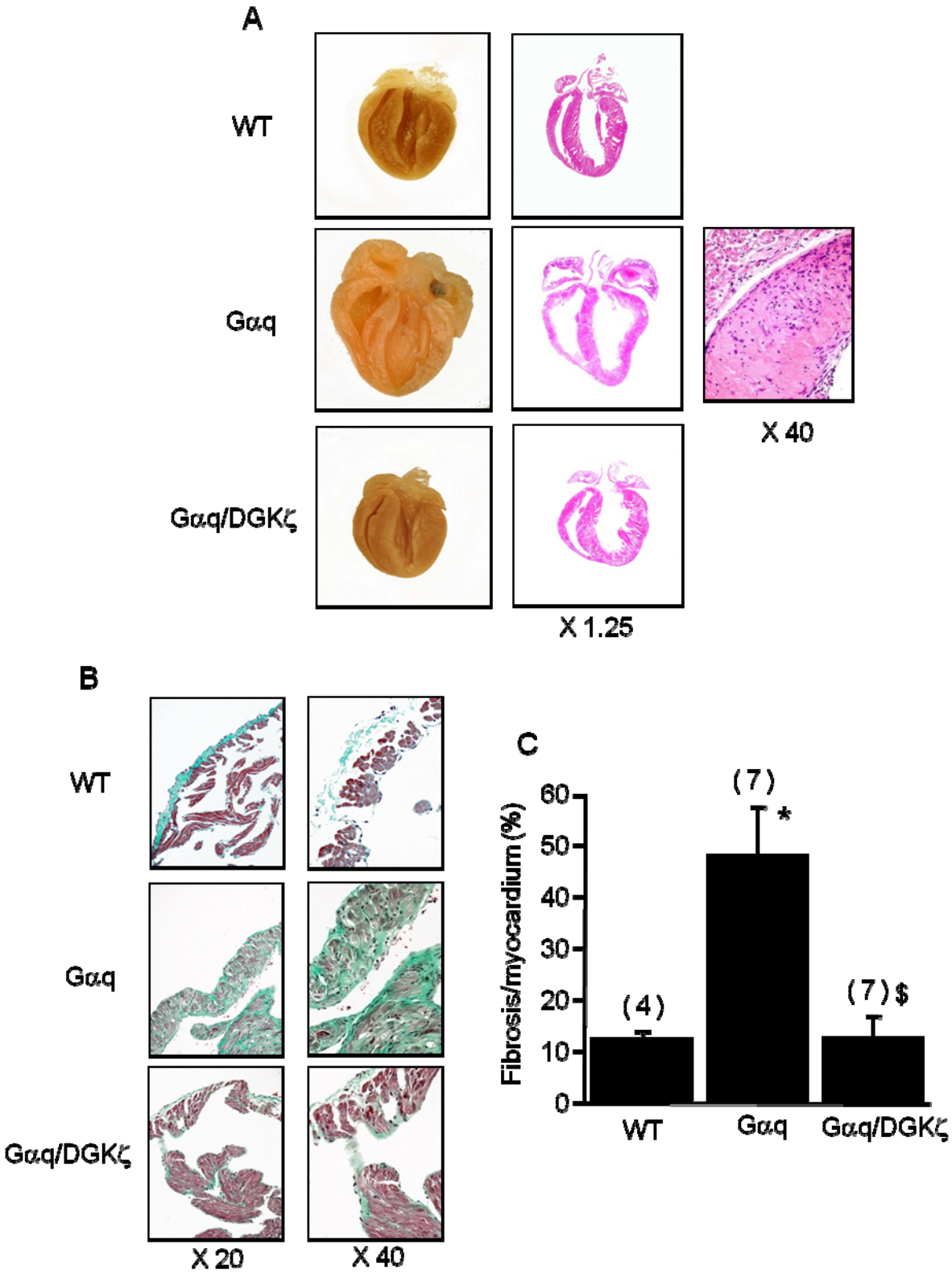
A
WT
Gαq
Gαq/DGKζ
X 40
X 1.25
B
WT
Gαq
Gαq/DGKζ
X 20
X 40
C
Fibrosis/myocardium (%)
60
50
40
30
20
10
0
(4)
(7)
*
(7) $
WT
Gαq
Gαq/DGKζ